Available online at www.sciencedirect.com
ScienceDirect
Trans. Nonferrous Met. Soc. China 27(2017) 1543−1550
Transactions of Nonferrous Metals Society of China
www.tnmsc.cn

Electrodeposition of multi-layer Pd−Ni coatings on 316L stainless steel and their corrosion resistance in hot sulfuric acid solution

Hui-zhong ZHANG, Yang LI, Yu ZUO, Xu-hui ZHAO, Yu-ming TANG

Beijing Key Laboratory of Electrochemical Process and Technology for Materials, Beijing University of Chemical Technology, Beijing 100029, China

Received 15 April 2016; accepted 7 July 2016

Abstract: Pd−Ni coating shows good corrosion resistance in strong corrosion environments. However, in complex aggressive environments, the performance of the coatings is limited and further improvement is necessary. The effects of the applied plating current density on the composition, structure and properties of Pd−Ni coatings were studied. By changing the current density in the same bath, multi-layer Pd−Ni coatings were prepared on 316L stainless steel. Scanning electronic microscopy, weight loss tests, adhesion strength, porosity and electrochemical methods were used to study the corrosion resistance of the films prepared by different coating methods. Compared with the single layer Pd−Ni coating, the multi-layer coatings showed higher microhardness, lower internal stress, lower porosity and higher adhesive strength. The multi-layer Pd−Ni coating showed obviously better corrosion resistance in hot sulfuric acid solution containing Cl^-.

Key words: Pd−Ni film; stainless steel; multi-layer film; electroplating; current density; corrosion resistance

1 Introduction

Stainless steels usually possess good corrosion resistance in natural environments due to the passive film on the surface. However, in some industrial environments such as sulfuric acid or acetic acid solutions at high temperature, severe corrosion may happen for stainless steels because the passive state is unstable or the passive film is damaged. The aggressive ions such as chloride ions in the environments would further accelerate corrosion of stainless steels [1−3], as a noble metal palladium coating can raise the potential of stainless steel substrates and promote passivation. There were many studies on palladium coatings on stainless steels, but most of the studies have paid attention to the properties of the coatings as absorption or catalysis materials for hydrogen [4]. In our previous studies [5,6], Pd alloy coatings were deposited on stainless steels by electroplating and brush plating. The Pd alloy coatings showed quite good corrosion resistance in strong reducing media and effectively protected the stainless steel substrate. However, in complex aggressive environments, the performance of the coatings is limited due to the effects of flow, erosion and abrasion by solid particles and further improvement is necessary.

Multi-layer films have attracted the interests of many authors in recent years because the film structure and the film properties including electric, optical, magnetic and mechanic properties may be controlled by different coating technologies, and multi-function films and the optimal result may be obtained by reasonable coating design [7,8]. Different grain sizes among different layers by electroplating may enhance the barrier effect of the coating to aggressive species, increasing the corrosion resistance [7,9]. Pd−Ni coating showed good corrosion resistance in strong reducing environments [10], as well as high microhardness and good adhesion to the stainless steel substrate [6]. In this work, the effects of current density on electroplated Pd−Ni film on 316L stainless steel were studied, and by controlling the current density in the same coating bath, multi-layer Pd−Ni coatings with good corrosion resistance were prepared originally. Compared with single layer Pd−Ni coating, the adhesion strength, microhardness and corrosion resistance of the multi-layer Pd−Ni coating are obviously improved, which showed that the multi-layer Pb−Ni coatings have obviously better

Corresponding author: Yu ZUO; Tel: +86-10-64423795; E-mail: zuoy@mail.buct.edu.cn
DOI: 10.1016/S1003-6326(17)60175-4

corrosion resistance in complex aggressive environment.

2 Experimental

2.1 Materials and film preparation

The substrate material was 316L stainless steel with the following chemical composition (mass fraction, %): Cr 16.80, Ni 13.50, C 0.02, Mn 1.40, Si 0.32, P 0.017, S 0.014, Mo 2.30, Fe Bal. The sample sizes were 20 mm × 10 mm × 2 mm. A mechanical surface preparation has been applied, using 240, 600 and 1000 grit abrasive papers, followed by an alkaline degreasing step in a solution consisting of 40−50 g/L Na_2CO_3, 40−50 g/L Na_3PO_4, 30−40 g/L NaOH, 40−50 g/L NaCl, 5−10 mL/L OP-10 (alkylphenol polyoxyethylene ether), at 80 °C for 30 min. After rinsing by hot water and deionized water, the acid cleaning activation process was carried out. The sample was cathodically polarized in the activation bath (40 mL/L H_2SO_4 + 120 g/L $(NH_4)_2SO_4$) at 40 °C for 8 min, and then rinsed with deionized water.

The Pd−Ni plating was carried out in the following bath at pH 8−9 and 45 °C: 10−18 g/L $PdCl_2$, 25−28 g/L $NiSO_4$, 15 mL/L $NH_3{\cdot}H_2O$ (28%), 50 g/L NH_4Cl, 35−50 g/L $Na_3C_6H_5O_7{\cdot}2\ H_2O$. A MD−30 power (Qunji Instruments Co., Xiamen, China) source was used, the plating current density was between 0.8 and 1.5 A/dm^2 and the time was 8 min. For multi-layer plating, at each current density the plating time was 2 min, and the whole plating time was still 8 min.

2.2 Measurements

A Hitachi S−4700 field emission scanning electron microscope (SEM) equipped with an energy dispersive X-ray spectrometer (EDX) was used to observe the micro-morphology and analyze the composition of the film. A D/max 2500VB2+/PC X-ray diffractometer was used to analyze the film structure. The grain size of the plated film was obtained by using the Scherrer equation: $d=0.9\lambda/(\beta\cos\theta)$, where d is the grain size, λ is the X-ray wave length, β is the peak width at half height, and θ is the diffraction angle.

The film microhardness was measured with an HM−2000 indentation hardness tester (Fischer). The load was 20 mN and the loading time was 20 s. For each sample, 10 parallel tests were carried out and the average value was obtained after taking out the maximum and the minimum values. The adhesion strength between the coating and the substrate was measured according to the standard ISO 4624−2002. The sample was made into disk with 30 mm in diameter and 2 mm in thickness, and the measuring instrument was a PosiTest Pull-Off adhesion tester (DeFelsko). The porosity of the coating was measured by a filter paper method, according to the standard QB/T 3823−1999 (The porosity measuring method for metallic coatings).

The internal stress in the coating was measured by cathodic bending method [11]. The coating was plated on one side of a copper foil. According to the deflection at the foil end, the internal stress S was calculated by following equation: $S=Et^2Z/(3dL^2)$, where E is elasticity modulus of the foil, t is the foil thickness, Z is the deflection at the foil end, d is the coating thickness and L is the foil length.

The corrosion resistance of the coatings has been determined using weight loss and polarization methods. The corrosion environment applied was 85 °C, 20% H_2SO_4 (mass fraction) solution with 200×10^{-6} NaCl (mass fraction), with stirring at 520 r/min. The testing time for weight loss was 168 h. After immersion test, the sample was ultrasonically cleaned in 10% HNO_3 solution for 10 min to remove the corrosion products, and then weighed. For each condition three samples were used and the average corrosion rate was obtained. A CS 350 electrochemical workstation was used to record the polarization curves of the coated samples. A saturated calomel electrode (SCE) was used as the reference electrode, and a long salt bridge was applied to making the SCE work at room temperature. The auxiliary electrode was a Pt foil and the coated sample was the working electrode. For each sample, the potential scanning started at a potential 200 mV negative to the open circuit potential (OCP) and ended at a potential 1500 mV positive to the OCP, with a scanning rate of 0.66 mV/s.

3 Results and discussion

3.1 Composition, structure and properties of single layer Pd−Ni coating

Figure 1 shows the Ni contents in Pd−Ni coating obtained at different plating current densities. With increasing current density, Ni content in the coating increased, indicating that the Ni content in coating may be controlled by changing the plating current density. It is known that the electro-deposition rate is affected by the applied current density, the overpotential and the rate of mass transfer [12−14]. The reduction potential of Pd is more positive than that of Ni. At lower current densities, Pd is preferentially deposited and the reaction is controlled by the activation process [12]. As the current density increases, both the deposition rates of Pd and Ni increase, but the deposition rate of Pd on the surface is influenced by the mass transfer of Pd ions from the bath body. Therefore, with the increase of the current density, the reduction of Pd becomes diffusion controlled and the deposition rate of Ni increases with the increase of current density [13,14]. With increasing Ni content, the

hardness and adhesion of the coating to the substrate may be raised [6,15,16]. Figure 2 shows the surface morphologies of the Pd−Ni coating at different current densities. It is seen that compact and homogeneous coatings were obtained under different current densities applied.

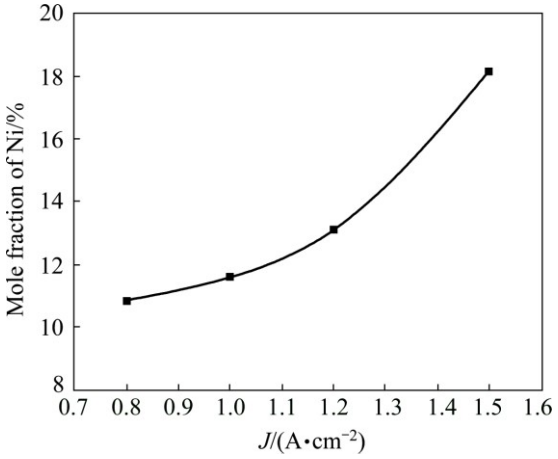

Fig. 1 Content of Ni in single layer Pd−Ni coating obtained under different current densities

Figure 3 shows the XRD patterns of the single layer Pd−Ni coating deposited at different current densities. In the figure the dotted vertical lines represent the standard diffraction peaks of Pd. It is seen that the diffraction patterns of Pd−Ni coatings are basically consistent with that of Pd, indicating that the Pd−Ni coatings remained the FCC structure of Pd. However, all the diffraction peaks of Pd−Ni coatings show small positive shift, suggesting that Ni atoms may dissolve in the crystal lattice of Pd to form a substitutional solid solution. The smaller Ni atoms in Pd lattice resulted in decreased lattice constant.

For the current densities between 0.8−1.2 A/dm^2, the preferred orientation of the Pd−Ni crystalline was (111), while when the current density increased to 1.5 A/dm^2, the preferred orientation was (200). The electrochemical reaction rate and the exchanging current density on different crystallographic planes are different [17−19], resulting in different growth rates on different planes. As the current density increased from 0.8 to 1.0, 1.2 and 1.5 A/dm^2, the calculated grain sizes by Scherrer equation were respectively 24.97, 23.93, 19.20 and 16.48 nm. The increased current density is helpful for raising the cathodic overpotential of the electrochemical deposition reaction, leading to increased driving force for the nucleation of grains, as the result, new crystal nucleus is easy to form and the average grain size would decrease [20,21].

Table 1 shows the properties of the single Pd−Ni coating obtained at different plating current densities. As the current density increased, the coating hardness increased from HV 368.3 to HV 453.8, and the internal stress in the coating also increased. According to the Hall−Petch equation, the relation between hardness and grain size follows $\sigma=\sigma_0+K_H d^{1/2}$ [22]. Hence, the higher current density leads to decreased grain size and increased hardness. Further, the smaller grains and higher dislocation density [21,23] also increase the internal stress in the coating.

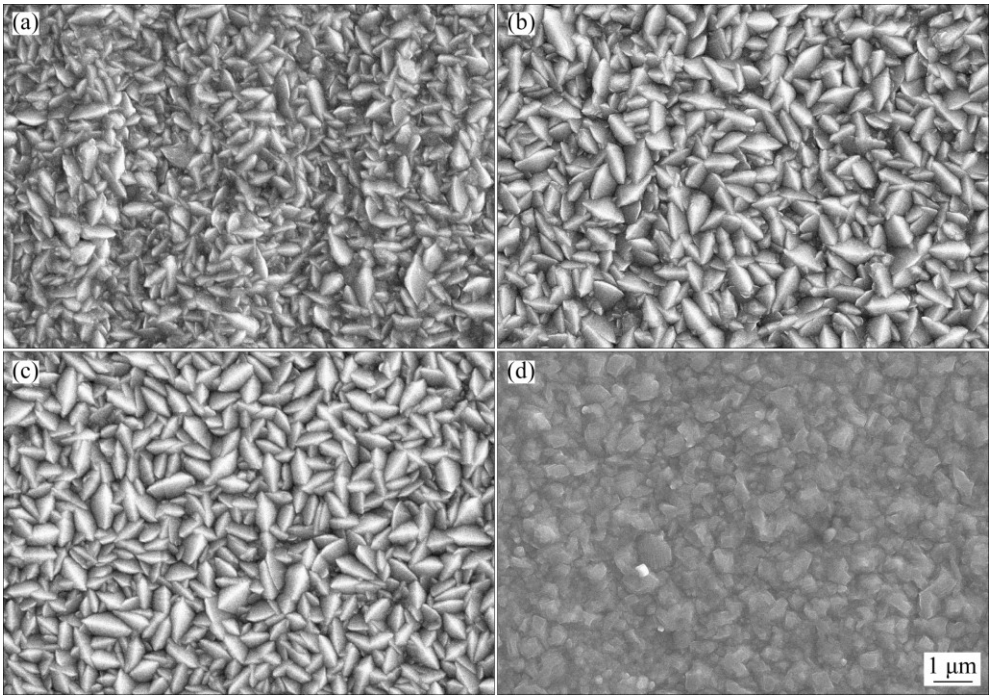

Fig. 2 SEM images of single layer Pd−Ni coating obtained under different current densities: (a) 0.8 A/dm^2; (b)1.0 A/dm^2; (c) 1.2 A/dm^2; (d)1.5 A/dm^2

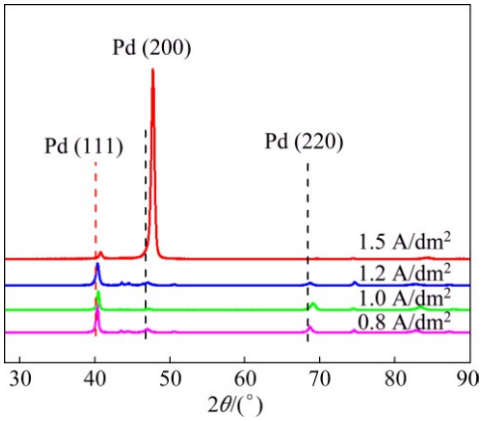

Fig. 3 XRD patterns of single layer Pd−Ni films obtained under different current densities

As the plating current density increased, the hydrogen evolution reaction rate increased, which may lead to higher porosity [24]. It is seen that at 0.8 A/dm^2 the coating showed the lowest porosity before or after immersion test. On the other hand, as the current density increased, the adhesive strength of the coating increased and reached the maximum value of 4.81 MPa at the current density of 1.2 A/dm^2. At higher current density the adhesive strength tended to decrease, which may be due to the increased internal stress [25,26].

3.2 Design and preparation of multi-layer Pd−Ni coating

According to the above results, the Ni content and properties of the coating may be controlled by changing the plating current density. When the current density was 1.5 A/dm^2 the microhardness of the Pd−Ni coating was the highest and when the current density was 1.2 A/dm^2 the adhesive strength was the best. Therefore, we selected 1.2 A/dm^2 to prepare the bottom layer and 1.5A/dm^2 to prepare the top layer, so as to obtain a multi-layer coating with high hardness and high adhesive strength to the substrate. On the other hand, multi-layers would increase the barrier effect [9]. Based on the above consideration, 7 kinds of multi-layer Pd−Ni coatings (A−G) were prepared and the current densities applied for different layers are shown in Table 2. Each multi-layer coating contains four coatings and the whole plating time was 8 min.

Table 3 shows the measured properties for the 7 multi-layer Pd−Ni coatings. The internal stress values of

Table 1 Properties of single layer Pd−Ni coating obtained under different current densities

J/(A·dm^{-2})	Microhardness (HV)	Internal stress/MPa	Porosity/cm^{-2}	Porosity after 72 h immersion/cm^{-2}	Adhesive strength/MPa	Adhesive strength after 48 h immersion/MPa
0.8	368.3	12.01	0.75	8.87	2.98	2.14
1.0	386.3	15.22	0.85	9.75	3.73	2.17
1.2	419.5	16.10	1.25	10.25	4.81	3.25
1.5	453.8	17.16	1.25	11.75	4.02	2.89

Table 2 Current densities applied for different layers in multi-layer Pd−Ni coatings

Layer	Current density/(A·dm^{-2})						
	A	B	C	D	E	F	G
Inside layer	1.2	1.2	1.2	1.2	1.2	1.2	1.2
Interlayer 1	0.8	0.8	1.0	1.0	1.5	1.5	1.5
Interlayer 2	1.0	1.2	0.8	1.2	0.8	1.0	1.2
Outside layer	1.5	1.5	1.5	1.5	1.5	1.5	1.5

Table 3 Characteristics of different multi-layer Pd−Ni coatings

Coating	Microhardness (HV)	Internal stress/MPa	Porosity/cm^{-2}	Porosity after 72 h immersion/cm^{-2}	Adhesive strength/MPa	Adhesive strength after 48 h immersion/MPa
A	408.6	11.19	0	3.25	4.56	4.06
B	418.4	12.38	0	4.2	4.48	3.82
C	389.4	15.36	0	6.15	4.37	3.42
D	423.6	12.87	0	3.6	4.42	3.78
E	392.6	15.89	0	6.8	4.25	3.25
F	410.8	14.43	0	3.75	4.38	3.36
G	436.7	13.16	0	2.75	4.69	4.13

all the 7 multi-layer coatings are less than 16 MPa, lower than that of the single layer Pd−Ni coating. The continuous change of gradient would result in less internal stress [25]. WANG et al [27] reported that internal stress was produced during the electro-deposition of nano Ni−Co coating, but continuous composition change in the coating may lead to the lowest internal stress. For all the multi-layer coatings, the hardness values are close to that of the outside layer, and the adhesive strength values are close to that of the inside layer. Also, because the multi-layers have better barrier effect to the aggressive species, the multi-layer coatings showed lower porosity than the single layer coating [7,9].

Immersion would result in increased porosity and decreased adhesive strength. It is seen in Table 3 that among the multi-layer coatings, coatings A and G remained higher adhesive strength and lower porosity after immersion test, indicating the best corrosion resistance.

3.3 Surface morphology, composition and corrosion resistance of multi-layer Pd−Ni coatings

Figure 4 shows the surface morphologies of the multi-layer coatings A and G. The coatings are compact and homogeneous. The cross section photos (Fig. 5) show that the coatings were closely bonded to the substrate and the thickness was 4−5 μm. Figure 6 shows the variations of Ni content in the two coatings from the internal interface. It is seen that the variation tendency of Ni contents in the coatings is consistent to the change of the current density, which confirms that the composition variation of the coatings is consistent to the previous coatings design.

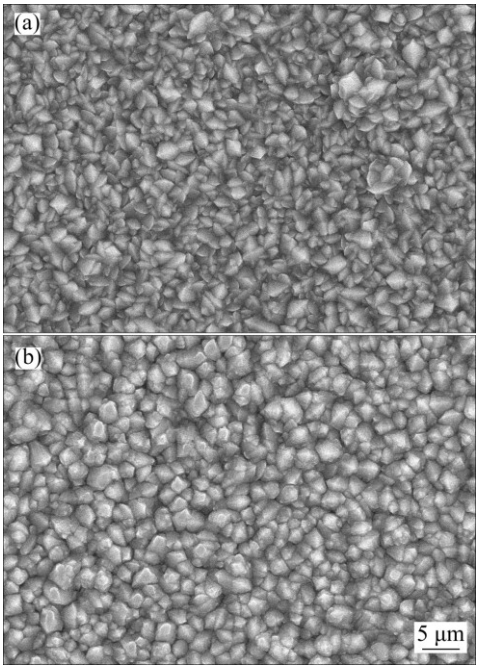

Fig. 4 Surface morphologies of multi-layer Pd−Ni films A (a) and G (b)

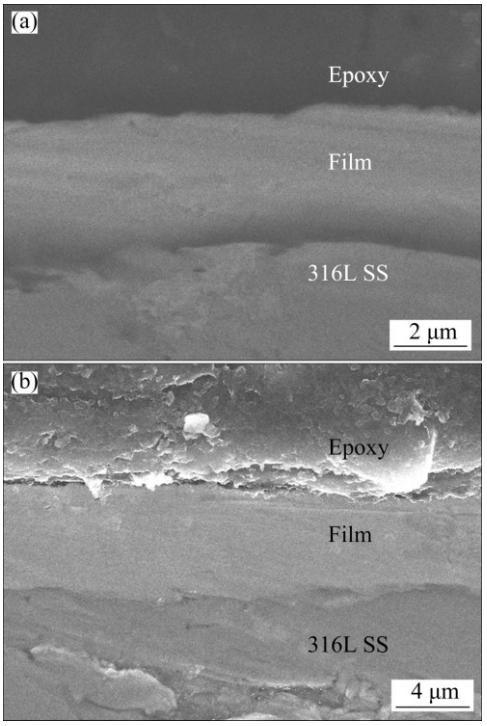

Fig. 5 Cross sections of multi-layer Pd−Ni films A (a) and G (b)

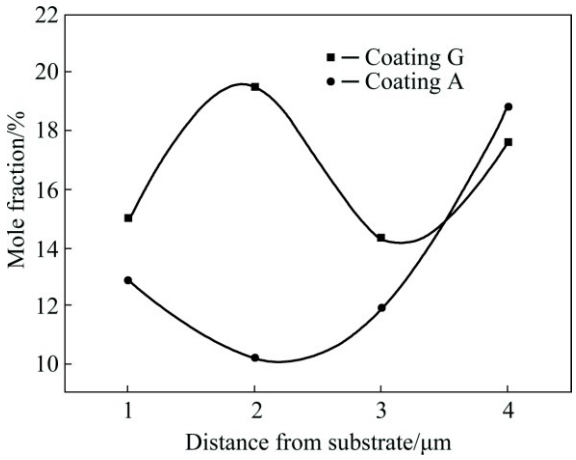

Fig. 6 Variations of Ni contents from internal interface in multi-layer Pd−Ni films A and G

Table 4 shows the mass loss results for different coatings samples in 20% H_2SO_4+200×10^{-6} NaCl solution at 85 °C and stirring speed of 520 r/min. The uncoated 316L stainless steel sample showed severe corrosion within 2 h. For the single Pd−Ni coated samples, the corrosion rates decreased by more than three orders of magnitude, indicating that the Pd−Ni coating can effectively protect the stainless steel substrate. However, the multi-layer coatings A and G showed better corrosion resistance, with lower corrosion rate values about one third of those of the single layer Pd−Ni coatings.

Table 4 Corrosion rates of different Pd−Ni coatings in 20% H_2SO_4+ 200×10^{-6} NaCl solution at 85 °C and 520 r/min

Sample	Testing time/h	Corrosion rate/($g\cdot m^{-2}\cdot h^{-1}$)	Corrosion phenomenon
316L SS	2	397.4	Severe corrosion
Single layer at 0. 8 A/dm^2	168	0.052	Intactness
Single layer at 1.0 A/dm^2	168	0.049	Intactness
Single layer at 1.2 A/dm^2	168	0.043	Intactness
Single layer at 1.5 A/dm^2	168	0.045	Intactness
Multi-layer coating A	168	0.018	Intactness
Multi-layer coating G	168	0.013	Intactness

Figure 7 shows potentiodynamic polarization curves of different Pd−Ni coatings samples in 20%H_2SO_4 + 200×10^{-6} NaCl solution at 85 °C and 520 r/min. Figure 7(a) indicates that the single layer Pd−Ni coating could raise the open circuit potential of the sample from −287 to 420 mV (vs SCE), and decrease the corrosion current density by more than three orders of magnitude. Figure 7(b) shows that the multi-layer Pd−Ni coating also raised the open circuit potential and further decreased the corrosion current density. After 76 h immersion, the open circuit potential of the single layer Pd−Ni coating shifted negatively to 158 mV, suggesting decreased corrosion resistance. The open circuit potentials of the multi-layer coatings A (217 mV) and G (327 mV) also shifted negatively after immersion, but were obviously more positive than that of the single coating. And the corrosion current densities of the multi-layer coatings A (4.2×10^{-6} A/cm^2) and G (1.7×10^{-6} A/cm^2) were also lower than that of the single layer Pd−Ni coating (6.3×10^{-6} A/cm^2) (Table 5), particularly for coating G. This result indicates that the multi-coatings have better corrosion resistance in contrast to the single layer coating, and the coating G showed the best results.

Figure 8 shows the surface morphologies of the single layer Pd−Ni coating after being immersed in 20% H_2SO_4+200×10^{-6} NaCl solution at 85 °C and 520 r/min stirring for 300 h. In some areas the coating has cracked and fallen off from the surface (Fig. 8(a)), and corroded grain boundaries on the bare substrate can be seen (Fig. 8(b)), indicating corrosion of the stainless steel substrate. Figure 9 shows the morphologies of the multi-layer coating G under the same environment after 300 h immersion. For most of the surface, the coating almost remained the original morphology (Fig. 9(a)), only a few localized defects could be found (Fig. 9(b)).

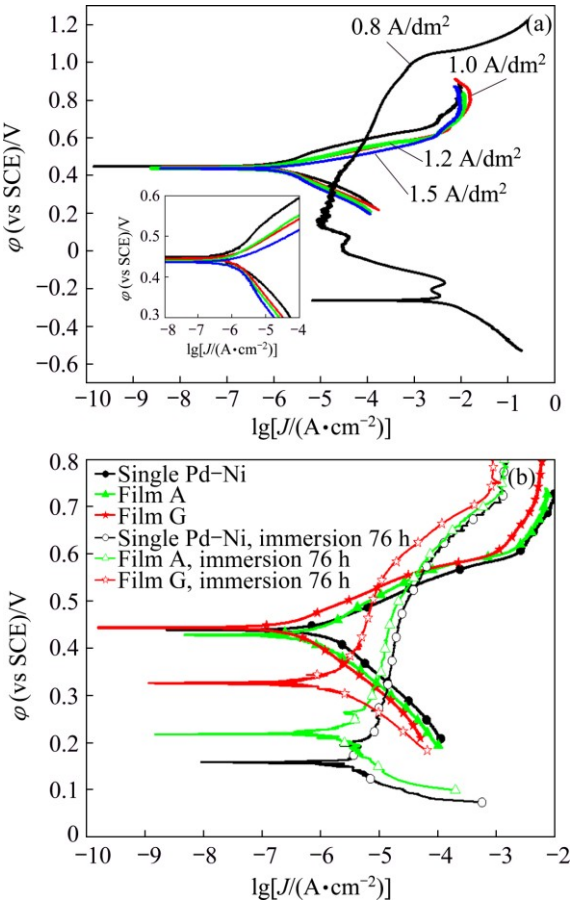

Fig. 7 Polarization curves of different films in H_2SO_4+ 200×10^{-6} NaCl solution at 85 °C and 520 r/min: (a) Pd−Ni with different current densities; (b) Different films before/after immersion for 76 h

Table 5 Electrochemical parameters for different multi-layer Pd−Ni films in Fig. 7(b)

Specimen	φ_c/mV	J_c/($A\cdot cm^{-2}$)
Single layer Pd−Ni film	438.8	7.2×10^{-7}
Multi-layer film A	427.4	6.8×10^{-7}
Multi-layer film G	442.5	3.6×10^{-7}
Multi-layer film G immersed for 76 h	324.7	1.7×10^{-6}
Multi-layer film A immersed for 76 h	217.3	4.2×10^{-6}
Single layer Pd−Ni film immersed for 76 h	158.8	6.3×10^{-6}

Different grain sizes of different layers may enhance the barrier effect and reduce the micro-pores in the multi-layer coating, hence increasing the corrosion resistance [7,9]. This result again confirms that the multi-layer Pd−Ni coating is more protective than single coating for stainless steels.

In conclusion, by changing the plating current density in the same bath, the obtained multi-layer Pd−Ni

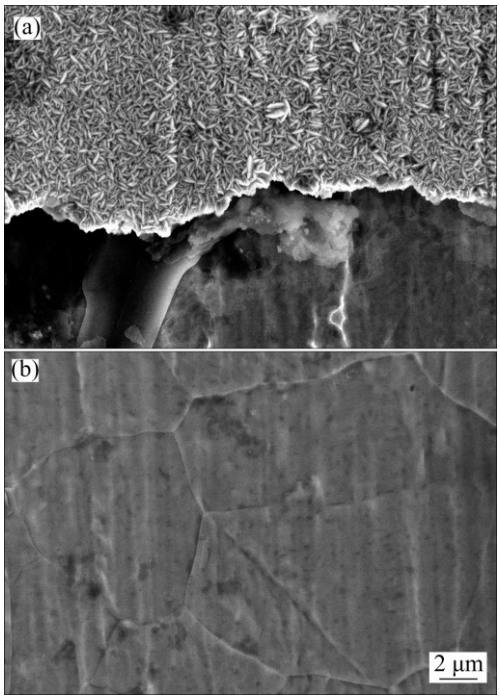

Fig. 8 SEM images of single Pd−Ni films after being immersed in H_2SO_4+ 200×10^{-6} NaCl solution at 85 °C and 520 r/min for 300 h: (a) Area of coating cracked and fallen from substrate surface; (b) Substrate of coating fallen off

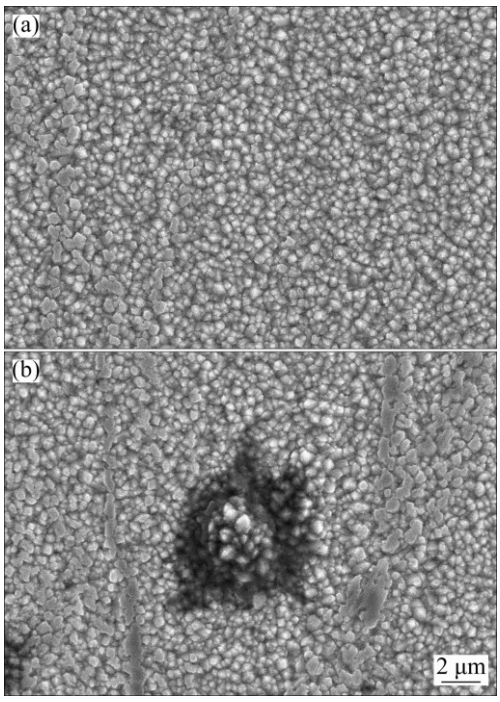

Fig. 9 SEM images of multi-layer Pd−Ni film G after being immersed in H_2SO_4+ 200×10^{-6} NaCl solution at 85 °C and 520 r/min for 300 h: (a) Most of coating surface; (b) Surface with localized defects

coating showed better properties than single layer Pd−Ni coating, including higher micro-hardness, higher adhesive strength, lower internal stress and lower porosity. The low porosity and high surface hardness obviously increase the corrosion resistance of the coating in flowing environments, and the high adhesive strength and low internal stress greatly improve the performance and lifetime of the coating. As a result, the multi-layer Pd−Ni coating possesses better corrosion resistance in complex severe corrosion environments.

4 Conclusions

1) The effects of plating current density on the composition and properties of Pd−Ni coatings were studied. It was shown that the Ni content and properties of the coating may be controlled by changing the plating current density. At the current density of 1.5 A/dm^2 the microhardness of the Pd−Ni coating was the highest and at the current density of 1.2 A/dm^2 the adhesive strength was the best.

2) By changing the current density in the same bath, multi-layer Pd−Ni coating was prepared on 316L stainless steel. Compared with the single layer Pd−Ni coating, the multi-layer coating showed higher microhardness, lower internal stress, lower porosity and higher adhesive strength.

3) Both single layer and multi-layer Pd−Ni coatings showed good protection for 316L substrate in 20% H_2SO_4+200×10^{-6} NaCl solution at 85 °C and 520 r/min. However, the multi-layer Pd−Ni coating showed obviously better corrosion resistance.

References

[1] TANG Jun-lei, ZUO Yu, TANG Yu-ming, XIONG Jin-ping. Composition and corrosion resistance of palladium film on 316L stainless steel by brush plating [J]. Transactions of Nonferrous Metals Society of China, 2012, 22(1): 97−103.

[2] XU Liang, ZUO Yu, TANG Jun-lei, TANG Yu-ming, JU Peng-fei. Chromium–palladium films on 316L stainless steel by pulse electrodeposition and their corrosion resistance in hot sulfuric acid solutions [J]. Corrosion Science, 2011, 53(11): 3788−3795.

[3] LI Si-rui, ZUO Yu, TANG Yu-ming, ZHAO Xu-hui. The electroplated Pd−Co alloy film on 316L stainless steel and the corrosion resistance in boiling acetic acid and formic acid mixture with stirring [J]. Applied Surface Science, 2014, 321: 179−187.

[4] LIU Fan, DENG Yi-da, HAN Xiao-peng, HU Wen-bing, ZHONG Cheng. Electrodeposition of metals and alloys from ionic liquids [J]. Journal of Alloys and Compounds, 2016, 654: 163−170.

[5] LI Si-rui, ZUO Yu. Erosion−corrosion behavior of Pd–Co and Pd–Cu films on 316L stainless steel in simulated PTA slurry environment [J]. Transactions of Nonferrous Metals Society of China, 2016, 26(1): 167−174.

[6] JU Peng-fei, ZUO Yu, TANG Jun-lei, HAN Zhong-zhi. The characteristics of a Pd−Ni/Pd−Cu double coating on 316 L stainless and the corrosion resistance in stirred boiling acetic and formic acids mixture [J]. Materials Chemistry and Physics, 2014, 144(3): 263−271.

[7] GU Chang-dong, LIAN Jian-she, LI Guang-yu, NIU Li-yan, JIANG Zhong-hao. High corrosion-resistant Ni−P/Ni/Ni−P multilayer

coatings on steel [J]. Surface & Coatings Technology, 2005, 197(1): 61−67.
[8] ZHENG H J, TANG F Q, LIM M, THOMAS R, ANIRUDDH M, WANG L Z, LU G Q. Electrochemical behavior of carbon-nanotube/cobalt oxyhydroxide nanoflake multilayer films [J]. Journal of Power Sources, 2009, 193(2): 930−934.
[9] XIAO Yu-guo, YIN Jian-jun, WANG Hui-li, SU Kai-min. Performance of multiple plating and coating layers of zinc alloy electronic components [J]. Materials Science & Technology, 2015, 23(6): 71−76. (in Chinese)
[10] WU Chang-lin, JU Peng-fei, ZUO Yu. Corrosion behavior of electroplated Pd−Ni film on 316L stainless steel, in aldehyde condensation solution [J]. Corrosion Protection in Petrochemical Industry, 2013, 30(5): 1−5. (in Chinese)
[11] CHEN Yan-rong, LONG Jin-ming, PEI He-zhong, HONG Jian-ping, SHI Xiao-zhao. Internal stress and Co content of pulse electrodeposited Ni−Co alloy coatings [J]. Plating and Finishing, 2009, 31(7): 1−3. (in Chinese)
[12] HAERIFAR M, ZANDRAHIMI M. Effect of current density and electrolyte pH on microstructure of Mn−Cu electroplated coatings [J]. Applied Surface Science, 2013, 284(11): 126−132.
[13] ZHAO Yuan-tao, CAI Fei, WANG Cheng-xin, CHAI Ze, ZHU Kai-yuan, XU Zhou, JIANG Chuan-hai. Investigation on the evolution of microstructure and texture of electroplated Ni−Ti composite coating by Rietveld method [J]. Applied Surface Science, 2015, 353(2): 1023−1030.
[14] PANEK J, BUDNIOK A. Production and electrochemical characterization of Ni-based composite coatings containing titanium, vanadium or molybdenum powders [J]. Surface & Coatings Technology, 2007, 201(14): 6478−6483.
[15] LIU Mei-hua, MENG Yi, ZHAO Yang, LI Fei-hua, GONG Yun-lan, FENG Lu. Electropolishing parameters optimization for enhanced performance of nickel coating electroplated on mild steel [J]. Surface and Coatings Technology, 2016, 286: 285−292.
[16] ZHANG Zi-ping, YU Gang, OUYANG Yue-jun. Studies on influence of zinc immersion and fluoride on nickel electroplating on magnesium alloy AZ91D [J]. Applied Surface Science, 2009, 255(17): 7773−7779.
[17] STOICHEV D S, TOMOV I. Influence of current density and temperature on the morphology and preferred orientation of electrodeposited copper coatings [J]. Electrochimica Acta, 1972, 17(11): 1955−1964.
[18] GU Min, YANG Zu-fang, HUANG Ling, YAO Shi-bing, ZHOU Shao-min. The formation of copper electrodeposits with highly preferred orientation and their surface morphology [J]. Acta Physico-Chimica Sinica, 2002, 18(11): 973−978.
[19] YE X P, de BONTE M, CELIS J P. Role of overpotential on texture, morphology and ductility of electrodeposited copper foils for printed circuit board applications [J]. Journal of the Electrochemical Society, 1992, 139(6): 1592−1600.
[20] RASHIDI A M, AMADEH A. Effect of electroplating parameters on microstructure of nanocrystalline nickel coatings [J]. Journal of Materials Science & Technology, 2010, 26(1): 82−86.
[21] SCHÜLER K, PHILIPPI B, WEINMANN M, MARX V M, VEHOFF H. Effects of processing on texture, internal stresses and mechanical properties during the pulsed electrodeposition of nanocrystalline and ultrafine-grained nickel [J]. Acta Materialia, 2013, 61(11): 3945−3955.
[22] WASEKAR N P, HARIDOSS P, SESHADRI S K, SUNDARARAJAN G. Influence of mode of electrodeposition, current density and saccharin on the microstructure and hardness of electrodeposited nanocrystalline nickel coatings [J]. Surface & Coatings Technology, 2016, 291: 130−140.
[23] NGUYEN V C, LEE C Y, CHEN F J, LIN C S, LIU T Y. Study on the internal stress of nickel coating electrodeposited in an electrolyte mixed with supercritical carbon dioxide [J]. Surface & Coatings Technology, 2012, 206(14): 3201−3207.
[24] LV Biao, WANG Xiao-he, HU Zhen-feng, XU Bin-shi. Effect of cathode movement on properties of nickel coatings electroplated at different current densities [J]. Electroplating & Finishing, 2013, 32(10): 5−9. (in Chinese)
[25] WANG Li-ping, GAO Yan, LIU Hui-wen, XU Tao. Study on electrodeposition of graded Ni−Co nanocrystalline alloys [J]. Electroplating & Finishing, 2004, 23(6): 5−7, 11. (in Chinese)
[26] MIYAMURA A, KANEDA K, SATO Y, SHIGESATO Y. Effects of internal stress on photocatalytic properties of TiO_2 films [J]. Thin Solid Films, 2008, 516(14): 4603−4608.
[27] WANG Li-ping, GAO Yan, XUE Qun-ji, LIU Hui-wen, XU Tao. Graded composition and structure in nanocrystalline Ni−Co alloys for decreasing internal stress and improving tribological properties [J]. Journal of Physics D: Applied Physics, 2005, 38(8): 1318−1324.

在 316L 不锈钢表面电沉积多层 Pd−Ni 膜层及其在高温硫酸中的耐蚀性能

张惠仲，李 阳，左 禹，赵旭辉，唐聿明

北京化工大学 材料电化学过程与技术北京市重点实验室，北京 100029

摘 要：不锈钢表面电镀 Pd−Ni 膜层在强腐蚀性溶液中对基体能起到良好保护作用，但膜层服役性能及寿命还需进一步提高。本文作者研究电流密度对 316L 不锈钢表面电沉积 Pd−Ni 膜层成分、组织和性能影响。在单一镀槽中通过控制电流密度在 316L 不锈钢基体上制备多种多层 Pd−Ni 膜层。采用扫描电子显微镜、失重实验、结合力、孔隙率和电化学方法研究不同制备工艺镀膜在强腐蚀溶液中的耐蚀性能。结果表明：相比单层膜层，多层膜层在保持较高显微硬度的同时，内应力明显减小，孔隙率显著降低，与基体的结合力提高；在含 Cl^-的高温硫酸环境中多层 Pd−Ni 膜层显示出更优异的耐蚀性能。

关键词：Pd−Ni 镀层；不锈钢；多层膜；电沉积；电流密度；耐蚀性能

(Edited by Wei-ping CHEN)